WALAILAK JOURNAL
http://wjst.wu.ac.th Engineering and Physical Sciences

Synergistic Use of Genetic Algorithm and Spectral Angle Mapper for Hyperspectral Band Selection of Roof Materials

Bahareh KALANTAR and Helmi Zulhaidi Mohd SHAFRI*

Department of Civil Engineering and Geospatial Information Science Research Centre (GISRC), Faculty of Engineering, Universiti Putra Malaysia, Selangor, Malaysia

(*Corresponding author's e-mail: helmi@upm.edu.my, bahare_kgh@yahoo.com)

Received: 12 March 2015, Revised: 11 November 2015, Accepted: 10 December 2015

Abstract

Hyperspectral data are valuable for urban studies because of the continuous narrow bands and high spectral resolution of such data. However, using hyperspectral data presents certain difficulties because of the high dimensionality. Hyperspectral data dimensionality should be reduced without losing the spectral detail of the data. In this study, we aim to assess the capability of hyperspectral data to discriminate roof materials and evaluate the feasibility of the genetic algorithm (GA) combined with the spectral angle mapper classification to identify significant bands that are effective in discriminating roof materials. The performance of GA was estimated using the overall classification accuracy. Field spectral reflectance from 4 types of roof materials in different conditions based on age (new and old) was collected using an Analytical Spectral Devices FieldSpec 3 Spectroradiometer with a wavelength range of 350 nm to 2500 nm. In this study, we confirm the potential of GA, with high overall classification accuracy (85 %), for the selection of significant bands that have valuable information to discriminate various types of roof materials. Overall, the results from the GA analysis show 3 principle locations of bands which are located at 517, 823 and 2008 nm in the visible, near infrared and shortwave region for discriminating different materials. This finding is in agreement with previous studies in determining the significant bands for man-made materials discrimination. Previous studies also discovered similar locations and ranges in the electromagnetic spectrum.

Keywords: Hyperspectral, band selection, roof materials, genetic algorithm, classification

Introduction

Urban environments consist of artificial and natural surfaces such as roads, grassy areas, and mixtures of concrete, steel, wood, stone, and other materials. Although remote sensing of urban areas can be complicated because of the different physical structures of roofing and paving materials, hyperspectral sensors are valuable tools for discriminating roof materials because of the high dimensionality over continuous narrow bands [1]. However, this high dimensionality causes difficulty in using hyperspectral data. Thus, hyperspectral data dimensionality should be reduced without losing the spectral detail of the data [2].

Two methods are employed to reduce the dimensionality of hyperspectral data. The first approach is applying band extraction. In this method, the original dataset is transformed before a definite number of bands are selected using the noise-adjusted principal component analysis (PCA) and Karhunen-Loeve transform approaches [3]. The most efficient method is band selection. This method selects a subgroup of original bands without effecting their physical meaning. As data do not change physically, band selection is preferable to band extraction [2]. In band selection, the interpretation of features is not as complex as that in band extraction [4]. Moreover, band extraction can have less classification accuracy because of transforming low-frequency information to the noisy bands [5]. Methods for band selection are divided

into 2 groups of supervised and unsupervised approaches. Unsupervised methods are computationally effective and fast and do not need training for ordering the bands. By contrast, supervised methods require training data and are more computationally demanding than unsupervised methods. Supervised approaches include artificial neural network (ANN), principal component analysis (PCA), and genetic algorithm (GA), whereas unsupervised approaches include information entropy measures as well as first and second derivatives [6]. It was determined that each of these approaches may be suitable for specific applications. The PCA and information entropy measures are useful when most information content about selection of bands is determined. However, derivative methods can be used to define features that are absorbed. The ANN measure is suitable for selection of bands that are specific to the characteristic of a target with minimum information layoff [6]. A new band selection method was formulated using a combination of 3 supervised and 7 unsupervised approaches under classification accuracy and computational requirement limitations [7]. The unsupervised methods, namely, first and second spectral derivatives, information entropy, spatial contrast, correlation, PCA, and spectral ratio, were used to rank hyperspectral bands. Meanwhile, the supervised methods, namely, regression, regression tree, and instance, were used for score ranking bands. Results showed that the highest 4 to 8 bands obtained by entropy followed by regression tree estimation were the best bands.

The GA is a common type of evolutionary optimization computation based on the concept of natural selection [8]. It was observed that GA used in band selection performs better than many other algorithms [9]. The GA-based band selector technique is a beneficial alternative to the floating search feature selection system [10]. It was also determined that GA adjusts a population of solutions simultaneously instead of a single solution such as the classical optimization procedure [11]. The combination of GA as a band selection tool with a well-known spectral angle mapper (SAM) was proposed based on the nearest neighbor classifier as fitness criterion to discriminate 16 tropical mangrove species. The result showed that the GA-based band selector can deal with the similarity of spectra in the species level [8]. The effectiveness of GA as a band selection tool for classification was also examined in remote sensing applications. The result showed that one of the optimal bands can achieve a better classification result [5]. Further to that a hybrid feature selection method based on GA and support vector machine (SVM) was proposed [12]. The method utilizes conditional mutual information for band grouping and applies the branch and bound algorithm through post-processing to filter out irrelevant band groups. The results showed that the proposed approach is competitive and operative. A combination of GA with SAM to identify a significant subset of bands that are sensitive to discriminate 13 broadleaved vegetation species was proposed by [13]. They determined that GA band selection has high overall classification accuracy. Moreover, the bands selected by GA are more valuable for the discrimination of vegetation species compared with bands selected randomly.

Until recently, only a few studies on band selection of man-made materials have been published despite the success of GA as a band selection tool for vegetation [8,13]. The applicability of GA could also be tested for man-made roofing materials. Therefore, in this study, we aim to evaluate the combination of GA and SAM for selecting significant bands that maintain spectral separability between different roof material classes from visible to shortwave infrared data (350 nm to 2400 nm; 2050 bands). The finding of this study will be a prerequisite for designing new multiband sensors for unmanned aerial vehicles (UAV) and configuring the bands for airborne hyperspectral urban mapping missions.

Materials and methods

The methodologies used in this study are discussed in this section. Several procedures conducted to achieve the objectives include data acquisition, preprocessing, and band selection combined with classification and accuracy assessment. Data acquisition involves spectral reflectance data collected from 4 types of roof materials, namely, clay, steel, concrete, and asbestos, using a spectroradiometer. Preprocessing includes conversion of the digital number (DN) into a reflectance value, conversion of the *.asd* format into an ASCII file of *.txt* format, and noise removal. The GA combined with the SAM classification was applied for band selection. Finally, the performance of GA was evaluated using the overall classification accuracy. The flowchart of this study is presented in **Figure 1**.

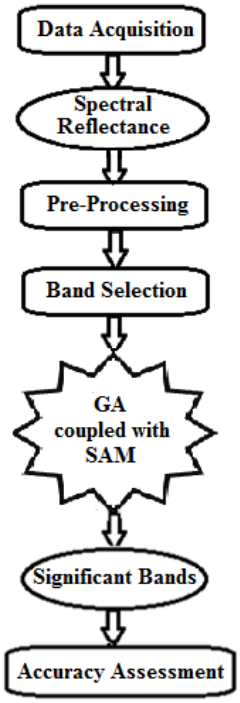

Figure 1 Methodology flowchart.

Data acquisition

Roof material sampling

Four types of roof materials in different conditions based on age (new and old) are used in this study. The materials are from the Faculty of Engineering, Universiti Putra Malaysia (UPM), located approximately 23 km south of Kuala Lumpur and 16 km north of Putrajaya with latitude N 1°24′ to N 2°32′ and longitude E 102°42′ to E 103°38′. **Figure 2** shows the location and image of the study area. **Figure 3** presents roof material sampling, including concrete, steel, clay, and asbestos, in different conditions based on age (old and new).

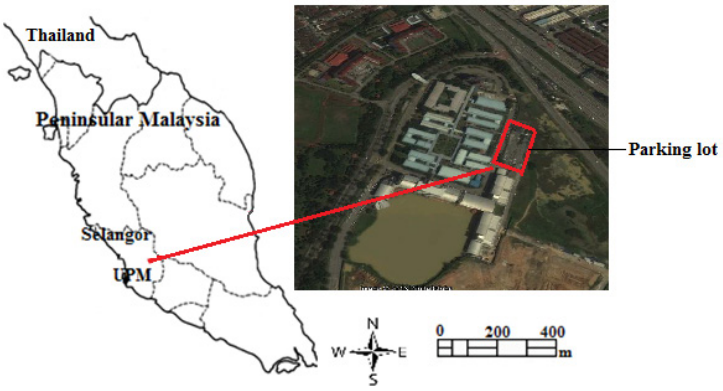

Figure 2 Location and image of the study area.

Figure 3 Samples of the roof materials (different types and conditions).

Spectral measurements

Field spectral reflectance of roof materials (different types and conditions) was collected using the ASD FieldSpec 3 Spectroradiometer at 10 am to 12 pm under clear sky condition in February and March 2013. The spectroradiometer has a spectral range of 350 nm to 2500 nm and a spectral resolution of 3 nm for a wavelength of 700 nm and 10 nm for bands from 1400 nm to 2100 nm. The data collected in the field included various types of roof materials, including steel, clay, asbestos, and concrete, in different conditions based on age (new and old). Thirty spectra were collected for each material at a height of 1 m and a field of view of 25° using bare fiber optic with 90° at nadir to achieve the target dimension with a spectral range between 350 nm and 2500 nm.

Table 1 shows the different types of roof materials used for spectral measurement in this study. The number of spectra from each target material was at least 30, which were collected using a 2150 band spectroradiometer. We considered a specific code for each target material based on their names.

Table 1 The roof materials used for spectral measurements. Thirty spectra were collected per roof material using a 2150 band spectroradiometer.

Roof materials	Code	Spectra number
Old asbestos	OA	30
Old clay	OCL	30
Old steel	OS	30
Old concrete	OC	30
New asbestos	NA	30
New clay	NCL	30
New steel	NS	30
New concrete	NC	30

The graph shown in **Figure 4** represents the average of the 30 spectra for each target material in reflectance value with a wavelength range of 350 nm to 2400 nm. In general, the spectral reflectance shape, intensity, width, and depth of absorption of the spectral curves are different in every target material. Notably, the spectral reflectance of roof materials was measured at different ages (new and old). The new and old types of spectral reflectance in asbestos are similar, except for the visible range. The difference between materials in the visible range is related to the color of the coating. Old and new clay have similar reflectances in the visible range because they have similar color of coating. Strong absorption on new and old clay observed in the visible range near 550 nm was caused by liquid water and hydroxyl groups [14]. The spectral reflectance of old and new concrete is completely different. New concrete has a low reflectance compared with old concrete because the coating of old concrete has a dark color. The spectral signatures of new and old steel are similar. However, new steel has high reflectance. The high spectral variability of the roof materials is due to the inconsistent mixture of ingredients in man-made materials and environmental variables, such as soil and water, which affect the reflectance spectra of the target materials. In summary, spectral curves varied between different materials because of the content of these materials and the color of their coating, although similarities in the absorption and reflectance of some wavelength ranges were observed.

Preprocessing

The DN of the raw data should be converted into reflectance values. Moreover, spectral data, which are in .asd format, are converted into ASCII in .txt format because data received from the spectroradiometer cannot be viewed using Microsoft Excel. Furthermore, hyperspectral data have more noise compared with multispectral data due to a low signal water vapor band and a transition at shortwave region [15], so we should deal with the noise. Denoising can be conducted by minimizing or eliminating the noise. In this case, the data range from 1350 nm to 1420 nm and from 1800 nm to 1950 nm; those greater than 2400 nm are eliminated because they render the feature shape of the spectra unrecognizable as a result of spectral stretch. **Figure 5** shows the spectral curves of new steel before and after noise removal.

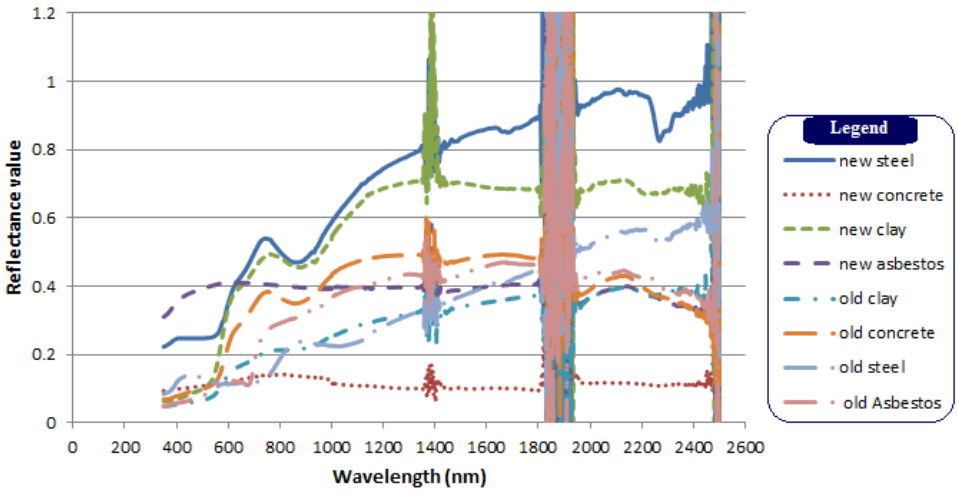

Figure 4 Mean spectral reflectance of different types of roof materials.

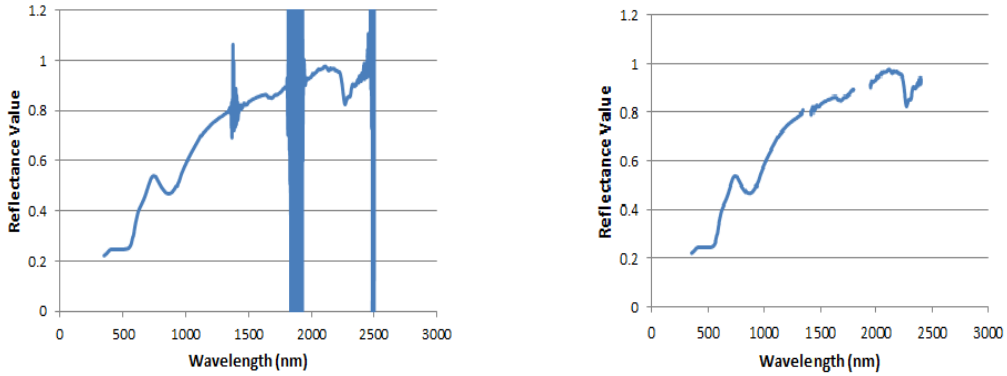

(a) (b)

Figure 5 Spectral curves of new steel (a) before and (b) after noise removal.

Band selection

Genetic algorithm

MATLAB software was used for processing in this study. GA is the technique used to optimize any type of data based on natural selection without evaluating all the candidate cases [16]. GA was determined to be a powerful tool for searching and solving complex problems as well as providing a population of solutions rather than a single solution [11]. GA produces an original population of individuals. Each individual is estimated using its overall fitness. New individuals are produced using 3 operations, namely, crossover, mutation, and selection. The production of new individuals continues until we obtain the individual that satisfies the conditions. A population contains chromosomes and each chromosome includes genes appointed to a band in this study [17].

In the crossover process, 2 chromosomes mate and create 2 offspring that have half of the character of one parent and the other half from another parent, which is called single-point crossover. Random mutations alter a single gene in the offspring chromosome, such that the characteristics of the offspring and parent are different.

One of the most important aspects of the GA is fitness function. In this study, we use the SAM classifier to estimate the fitness values of the chromosome population during processing. The SAM is a physically based spectral classification that uses an n-dimensional angle to match the pixel to the reference spectra [18]. The algorithm determines the spectral similarity between 2 spectra by calculating the angle between them. For calculating the fitness function, half of the spectra of each target (15 spectra per target) are used for training purposes and the remaining half for testing purposes. The reference spectrum for each target is calculated using the average spectrum of the training dataset [13].

The selection is conducted based on the fitness values. In this study, the fitness score is calculated based on the overall classification accuracy from the SAM classification. Chromosomes with higher classification accuracy have a higher chance of being selected for the next generation.

Significant bands

The GA is used to select the significant bands based on the overall classification accuracy of the SAM. The bands with higher overall classification accuracy have a higher chance of being selected. There is valuable information in significant bands compared with the other bands.

Accuracy assessment

Accuracy assessment is an important aspect of classification, which is normally evaluated by comparing the classification data with the reference data. Accuracy assessment reflects the difference between our classification data and the reference data. Overall classification accuracy was applied to estimate the performance of GA combined with SAM as band selection method.

Table 2 Forty best chromosomes with fitness scores (%).

Chromosome no.	Genes (nm)					Fitness scores (%)
1	352	392	750	766	928	87.5
2	391	391	715	914	2386	86.66
3	416	592	682	804	879	86.66
4	361	390	400	749	943	87.5
5	352	476	614	731	739	86.66
6	363	531	675	686	733	86.66
7	359	556	670	828	891	86.66
8	490	660	1970	2103	2298	84.16
9	468	498	501	746	855	86.66
10	373	461	605	693	892	87.5
11	466	1268	2011	2067	2310	78.33
12	540	668	679	780	955	86.66
13	429	445	535	547	692	86.66
14	446	474	680	848	934	87.5
15	493	510	621	688	933	86.66
16	415	512	667	748	2341	87.5
17	411	496	1222	1975	2365	82.5
18	404	802	1799	2192	2397	80
19	405	479	623	726	731	86.66
20	436	494	1301	2314	2370	79.16
21	494	1245	2018	2282	2324	78.33
22	354	397	416	735	1982	85.83
23	440	449	543	601	714	86.66
24	384	629	638	784	988	87.5
25	354	402	499	647	728	87.5
26	369	426	504	722	900	87.5
27	435	487	736	994	2010	86.66
28	358	499	746	904	927	87.5
29	466	493	661	739	821	86.66
30	391	634	756	817	943	87.5
31	396	691	786	986	999	87.5
32	451	750	773	793	847	87.5
33	355	459	736	755	916	87.5
34	489	1291	1978	2123	2310	78.33
35	438	518	677	901	944	86.66
36	475	738	782	833	837	87.5
37	387	528	649	756	865	86.66
38	490	735	789	841	974	87.5
39	354	384	627	725	802	87.5
40	382	418	758	877	1970	85

Results and discussion

Preliminary parameters are organized as follows: population size = 1000, number of generations = 500, crossover rate = 100 %, and mutation rate = 1 %. The fitness function was determined based on the SAM classification accuracy during the evolution procedure. The consistency of the result was checked by running the GA 40 times.

Table 2 presents the winning chromosomes of every run with the proportion of fitness scores. Notably, the chromosome size for the classification of different types of roof materials was 5. The fitness scores of all 40 chromosomes were greater than 78 %. The highest fitness score was at the 87 % level of classification accuracy. Then, genes were grouped into 3 waveband regions of visible (380 - 700 nm), near infrared (700 - 1000 nm), and shortwave infrared (1000 - 2400 nm) based on the mean and standard deviation.

Table 3 shows a summary of the selected genes (bands) in 3 spectral regions. In general, wavelength ranges were selected based on the mean wavelength location and standard deviation. Notably, 3 principal locations of 40 runs were located at 517, 823, and 2008 nm. The number of genes was calculated to be 48, 41 and 22 for the visible, near infrared and shortwave infrared region, respectively. In conclusion, the significant bands based on GA were grouped into 3 spectral regions based on the mean and standard deviation.

The graph in **Figure 6** shows the significant bands (highlighted parts) based on the reflectance value between wavelengths of 350 nm and 2400 nm obtained using GA. In general, the significant bands were grouped into 3 spectral regions of visible, near infrared, and shortwave infrared. In the visible area, the 417 - 617 nm range was selected as the significant band. For the second spectral (near infrared) region, the 737 - 909 nm range was considered as the significant band. Moreover, the 1633 to 1799 and 1951 to 2383 nm range was selected as the significant band in the shortwave infrared region. In summary, we observed that significant bands for best separability of room materials appear in almost all parts of the spectrum, especially in the visible and shortwave infrared region.

Table 3 Grouping of selected genes (bands) in 3 spectral regions.

Spectral region	Mean (spectral band, nm)	Standard deviation (nm)	No. of genes (bands)	Mean ± standard deviation	Wavelength range (nm)
Visible	517	100	48	517±100	417 to 617
Near infrared	823	86	41	823± 86	737 to 909
Short wave infrared	2008	375	22	2008± 375	1633 to 1799 1951 to 2383

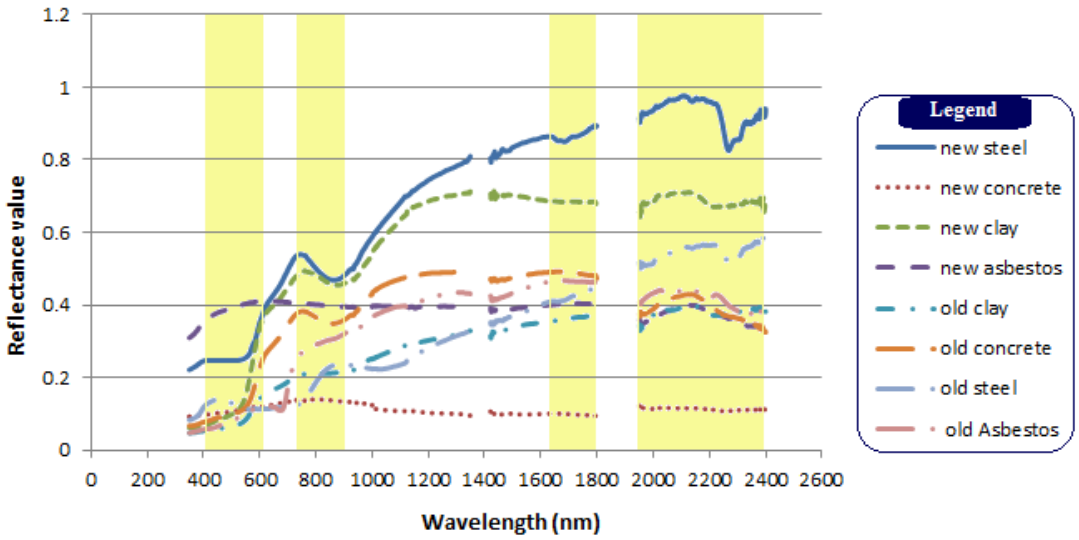

Figure 6 Significant bands based on GA.

Table 4 shows a confusion matrix of the average of 40 runs for 4 different roof materials in different conditions based on age (new and old). In general, the overall classification accuracy of the training and testing datasets was 100 and 85.78 %, respectively. Notably, the overall classification accuracy in the testing dataset is not 100 % because some materials were not classified correctly. For instance, new steel was misinterpreted as old clay (OCL) and old concrete (OC) in the majority of the runs. In summary, the 2 tables show the overall classification accuracy for the testing and training datasets, with the average confusion matrix of 40 runs.

Table 4 The average of confusion matrix of 40 runs for the training and testing dataset.

	NCL	NS	NA	NC	OA	OCL	OC	OS
NCL	15	0	0	0	0	0	0	0
NS	0	15	0	0	0	0	0	0
NA	0	0	15	0	0	0	0	0
NC	0	0	0	15	0	0	0	0
OA	0	0	0	0	15	0	0	0
OCL	0	0	0	0	0	15	0	0
OC	0	0	0	0	0	0	15	0
OS	0	0	0	0	0	0	0	15

Total accuracy classification of training dataset = 100 %

	NCL	NS	NA	NC	OA	OCL	OC	OS
NCL	15	0	0	0	0	0	0	0
NS	2.7	0	0	0	0.425	4.975	6.9	0
NA	0	0	15	0	0	0	0	0
NC	0	0.275	0.875	13.85	0	0	0	0
OA	0	0	0	0	15	0	0	0
OCL	0	0	0	0	0.075	14.925	0	0
OC	0	0	0	0	0	0.325	14.675	0
OS	0	0.325	0	0	0.075	0.1	0	14.5

Total accuracy classification of testing dataset = 85.78 %

In this study, we assessed the capability of hyperspectral remote sensing data in analyzing the different types of roof materials. The physical structure and chemical content of the material makes it possible to discriminate different roof materials. The color of the coating has an effect on the spectral curves. Black coatings cause a more similar spectral reflectance to gray coating compared with brown and blue color coatings. The same materials at different ages (new and old) and environmental conditions could be separated by comparing their spectral reflectance shapes. The results of the field spectra comparison confirm that the hyperspectral data are able to discriminate different roof materials. Moreover, we investigated the applicability of GA for selecting significant bands to discriminate different roof materials in different conditions. GA has been extensively used for plant species discrimination. However, only a few studies on urban areas have been published. The result of this study shows overall classification accuracy greater than 78 % (**Table 2**), such that band selection by GA was meaningful.

One important aspect that affects the performance of GA is the fitness function, which is typically estimated based on the training samples. In this study, the classification accuracy of the SAM was applied to calculate the fitness scores, although other well-known classifiers could replace SAM, such as SVM [8]. The outcomes show 3 principal locations of significant bands, namely, 517, 823, and 2008 nm, for discriminating roof materials in 3 spectral regions of visible, near infrared, and shortwave infrared, respectively. The spectral ranges of 417 - 617 nm, 737 - 909 nm, 1633 - 1799 and 1951 - 2383nm, which are selected based on the mean and standard deviation of winning genes (bands) on 40 runs by GA, are considered as the significant range bands. In the visible and shortwave regions, more significant bands were compared with the near infrared region. The GA was evaluated through accuracy assessment of the training and testing datasets.

Accuracy classifications were 85 and 100 % for the testing and training datasets, respectively. By contrast, some materials were misinterpreted because of similar absorption. The highest accuracy classification confirmed the potential of GA as an optimal band selection method for discriminating different types of roof materials.

Conclusions

In conclusion, this study confirmed the capability of hyperspectral data with high spectral resolution collected using a ASD FieldSpec 3 Spectroradiometer to discriminate various types of roof materials in different conditions based on age (new and old). Moreover, GA has the potential to select significant bands with valuable information on the materials. The performance of GA was estimated with an overall classification accuracy of 85 %. Overall, the result from the GA analysis shows that the principle bands are located at 517, 823 and 2008 nm in the visible, near infrared and shortwave region respectively to discriminate different types and conditions of materials. This finding is in agreement with previous studies conducted by [15,19,20] in determining the significant bands for man-made materials discrimination. Previous studies as mentioned also discovered similar locations and ranges in the electromagnetic spectrum. Future work could apply the band selected to airborne hyperspectral data to discriminate different roof materials. The development of sensors for UAV can also benefit from using the optimal bands to produce a light and cost-effective sensor. A toolbox for processing field spectrum data can also be developed to assist non-experts in hyperspectral remote sensing to extract useful information effectively.

Acknowledgement

The authors acknowledge the financial supports provided by the Ministry of Education (MOE) Malaysia through Fundamental Research Grant Scheme (FRGS) and the Research University Grant Scheme (RUGS) by Universiti Putra Malaysia (UPM).

References

[1] HZM Shafri, E Taherzadeh, S Mansor and R Ashurov. Hyperspectral remote sensing of urban areas: An overview of techniques and applications. *Res. J. Appl. Sci. Eng. Tech*. 2012; **4**, 1557-65.
[2] X Hao and JJ Qu. Fast and highly accurate calculation of band averaged radiance. *Int. J. Remote Sens.* 2009; **30**, 1099-108.
[3] AA Green, Berman M, P Switzer and MD Craig. A transformation for ordering multispectral data in terms of image quality with implications for noise removal. *IEEE Trans*. *Geosci. Remote Sens.* 1988; **26**, 65-74.
[4] C Conese and F Maselli. Selection of optimum bands from TM scenes through mutual information analysis. *ISPRS J. Photogramm. Eng. Remote Sens*. 1993; **48**, 2-11.
[5] X Zhang and M Pazner. Comparison of lithologic mapping with ASTER, hyperion, and ETM data in the southeastern Chocolate Mountains, USA. *Photogramm. Eng. Remote Sens*. 2007; **73**, 555-61.
[6] M Kudo and J Sklansky. Comparison of algorithms that select features for pattern classifiers. *Pattern Recognit*. 2000; **33**, 25-41.
[7] P Bajcsy and P Groves. Methodology for hyperspectral band selection. *Photogramm. Eng. Remote Sens*. 2004; **70**, 793-802.
[8] C Vaiphasa, AK Skidmore, WF de Boer and T Vaiphasa. A hyperspectral band selector for plant species discrimination. *ISPRS J. Photogramm. Eng. Remote Sens*. 2007; **62**, 225-35.
[9] W Siedlecki and J Sklansky. A note on genetic algorithms for large-scale feature selection. *Pattern Recognit. Lett*. 1989; **10**, 335-47.
[10] S Yu, S De Backer and P Scheunders. Genetic feature selection combined with composite fuzzy nearest neighbor classifiers for hyperspectral satellite imagery. *Pattern Recogn. Lett*. 2002; **23**, 183-90.
[11] H Fang, S Liang and A Kuusk. Retrieving leaf area index using a genetic algorithm with a canopy radiative transfer model. *Remote Sens. Environ*. 2003; **85**, 257-70.
[12] S Li, H Wu, D Wan and J Zhu. An effective feature selection method for hyperspectral image classification based on genetic algorithm and support vector machine. *Knowledge-Based Syst*. 2011; **24**, 40-8.
[13] S Ullah, TA Groen, M Schlerf, AK Skidmore, W Nieuwenhuis, C Vaiphasa. Using a genetic algorithm as an optimal band selector in the mid and thermal infrared (2.5 - 14 μm) to discriminate vegetation species. *Sensors* 2012; **12**, 8755-69.
[14] NEM Nasarudin and HZM Shafri. Development and utilization of urban spectral library of remote sensing of urban environment. *J. Urban. Environ. Eng*. 2011; **5**, 44-56.
[15] M Herold, DA Roberts, ME Gardner and PE Dennison. Spectrometry for urban area remote sensing-Development and analysis of a spectral library from 350 to 2400 nm. *Remote Sens. Environ*. 2004; **91**, 304-19.
[16] JH Holland. *Adaptation in Natural and Artificial System: An Introductory with Application to Biology, Control and Artificial Intelligence*. University of Michigan Press, Ann Arbor, 1975.
[17] DE Golberg. *Genetic Algorithms in Search, Optimization, and Machine Learning*. Addison-Wesley, Boston, USA, 1989.
[18] F Kruse, A Lefkoff, J Boardman, K Heidebrecht, A Shapiro, P Barloon and AFH Goetz. The spectral image processing system (SIPS)-interactive visualization and analysis of imaging spectrometer data. *Remote Sens. Environ*. 1993; **44**, 145-63.
[19] M Herold, ME Gardner and D Roberts. Spectral resolution requirements for mapping urban areas. *IEEE Trans. Geosci. Remote Sens.* 2003; **41**, 1907-19.
[20] E Ben-Dor, N Levin and H Saaroni. A spectral based recognition of the urban environment using the visible and near-infrared spectral region (0.4 - 1.1 μm). A case study over Tel-Aviv, Israel. *Int. J. Remote Sens.* 2001; **22**, 2193-218.